Fast Neutron Induced Nuclear Counter Effect in Hamamatsu Silicon PIN Diodes and APDs

Liyuan Zhang, *Member, IEEE*, Rihua Mao, *Member, IEEE*, and Ren-Yuan Zhu, *Senior Member, IEEE*

Abstract—Neutron induced nuclear counter effect in Hamamatsu silicon PIN diodes and APDs was measured by irradiating fast neutrons from a pair of ^{252}Cf sources directly to these devices. It was found that the entire kinetic energy of these neutrons may be converted into electron signals in these devices, leading to anomalous signals of up to a few million electrons in a single isolated calorimeter readout channel. Signals of such amplitude represent equivalent energy of several hundred GeV and a few GeV for PWO and LSO/LYSO crystals respectively assuming the corresponding light yields of 4 and 800 p.e./MeV. The overall rate of the neutron induced nuclear counter effect in APDs is found to be more than an order of magnitude less than that in PIN diodes. Increasing the APD gain was also found to reduce the neutron induced nuclear counter effect. An intelligent front-end chip capable of selecting un-contaminated signal is proposed to eliminate completely the nuclear counter effect without significant cost increase.

Index Terms—Calorimeter, crystal, fast neutron, neutron, nuclear counter effect, photo-detector, silicon .

I. INTRODUCTION

BECAUSE of their immunity to magnetic fields silicon based readout devices, such as silicon PIN photo-diodes and avalanche photo-diodes (APDs), are widely used as photo-detectors for reading out scintillation photons. Modern crystal calorimeters, for example, use either PIN diodes or APDs as the readout device. These photo-detectors are located in the middle of particle showers during experimental data taking, where charged particles and neutrons are produced copiously. While the nuclear counter effect caused by minimum ionizing charged particles in PIN diodes [1] and APDs [2] is well understood it is less studied for neutrons. Thermal or fast neutrons are frequently used to irradiate various silicon based photo-detectors. The main purpose of these studies, however, is to investigate the neutron induced radiation damage effects in these devices, e.g., the degradation of the dark current etc. Fast neutron induced pulse height spectrum was reported for a Hamamatsu PIN diode S3590-02 [3] with a 200 μm thick depletion layer as a possible neutron sensor. This device, however, has a much reduced thickness as compared to the Hamamatsu

The authors are with the California Institute of Technology, Pasadena, CA 91125 USA (e-mail: zhu@hep.caltech.edu; liyuan@hep.caltech.edu; maorh@hep.caltech.edu).

S2744-08 PIN diodes with a 300 μm thick depletion layer which are widely used in high energy physics experiments. No previous publication was found for neutron induced pulse height spectrum in APDs.

GEANT simulations show that fast neutrons are produced copiously at hadronic colliders, such as the LHC, with an energy spectrum peaked at a few MeV [4]. A flux of about 10^5 cm^{-2}s^{-1} is expected for the Hamamatsu S8664-55 silicon APDs, which are used as the photo-detectors for the CMS barrel PWO electromagnetic calorimeter (ECAL), when the LHC is running at the designed LHC luminosity of 10^{34} cm^{-2}s^{-1} with 7 TeV beam energy [4]. Neutrons can also be produced through photonuclear reactions from bremsstrahlung photons via the Giant Dipole Resonance (GDR) mechanism with an energy spectrum similar to and a rate of about 1% of that from hadrons [5].

Interactions between neutrons and photo-detector material are well understood. For fast neutrons, the dominant process with cross section of up to ten barns is elastic neutron-nucleus collision through which a neutron transfers a fraction of its kinetic energy to a nucleus. The charged nucleus subsequently deposits its kinetic energy in the photo-detector through ionization and creates electron–hole pairs at a rate of 3.62 eV per pair. Up to a few million electrons may be induced when the entire kinetic energy of the fast neutron is converted to electron–hole pairs in a photo-detector. The corresponding equivalent energy of neutron induced electron signals in a calorimeter cell depends on crystal's light yield. Signals of a few million electrons correspond to several hundreds GeV for a PWO ECAL with typical light yield of 4 p.e./MeV for calorimeter size crystals with APD readout. Signals of the same amplitude would correspond to a few GeV for LSO/LYSO crystals with typical light yields of 800 p.e./MeV with APD readout. Since the upper energy scale is also about two hundred times different between the LHC and the proposed SuperB collider the impact of such signals to the physics output is comparable between the CMS PWO calorimeter at the LHC and the proposed SuperB forward LSO/LYSO calorimeter [6].

Since the beginning of LHC operations in late 2009 anomalous signals have been observed in single isolated readout channels in the CMS barrel PWO ECAL, where Hamamatsu S8664-55 silicon APDs are used as the photo-detector [7]. Contrary to the showering photons and electrons, these anomalous signals are characterized by little or no energy observed in their neighbors. They appeared at a rate of about 10^{-3} in minimum bias events [7]. Their amplitude was found to be up to several hundred GeV equivalent in the extreme cases. Strategies have been developed by CMS to reduce their impact on the physics output [7]. Effort was made to eliminate events contaminated by the anomalous signals using event topology,

such as the spatial energy distribution and the event timing etc. For 2010 LHC runs at 3.5 TeV beam energy and about 10^{32} cm^{-2}s^{-1} luminosity the particular topology of these events allow a majority of the anomalous signals be removed at the trigger stage without affecting calorimeter performance for real physics. It, however, is clear that such rejection would be less effective when the beam energy and luminosity of the LHC increase because of the increased event energy and overlapping minimum bias and pile-up events. It is also clear that such effects can be completely eliminated by multiple photo-detectors with independent readout channels for a single calorimeter cell. Hardware solution would thus be preferred to make sure there was no contamination in physics analysis.

These anomalous signals observed by the CMS ECAL are caused by signals induced directly by shower particles in photo-detectors, conventionally called nuclear counter effect. Since the nuclear counter effect caused by minimum ionizing particles would not produce signals of such amplitude it was suspected that these signals were caused by heavily ionizing nuclei, which receive their kinetic energies through collisions with neutrons. To investigate neutron induced nuclear counter effect in silicon photo-detectors fast neutrons from a pair of ^{252}Cf sources were used to irradiate the following devices.

1) A Hamamatsu S2744-08 PIN diode with an active area of 1×2 cm^2 and a 300 μm thick depletion layer.
2) A pair of Hamamatsu S8664-55 APDs with an active area of $2 \times 5 \times 5$ mm^2, a 5 μm thick active layer before the avalanche amplification and a 45 μm layer of silicon with a low gain behind the avalanche region [8].

Both photo-detector chips have a 500 μm thick epoxy coating at the top of the device surface and are bounded to ceramic package with conductive epoxy of several tens of μm thick [9]. While Hamamatsu S2744-08 PIN diodes are used as photo-detectors for the $BaBar$, BELLE and BES III CsI(Tl) calorimeters, Hamamatsu S8664-55 APDs are used for the CMS PWO calorimeter. Both are candidate photo-detectors for the proposed SuperB LSO/LYSO calorimeter [6].

Fast neutron induced pulse height spectra in these photo-detectors were measured. Section II describes the experimental setup, the neutron sources used in this investigation and the calibrations of these photo-detectors for the absolute electron numbers and the APD gains. The neutron induced pulse height spectra measured by APDs and PIN diodes are presented in Section III. Also presented in this section are the possible background pulse hight spectra by X-rays and low energy γ-rays. Section IV describes a proposed hardware solution to eliminate the nuclear counter effect completely for future calorimeters using silicon photo-detectors. Section V provides a brief summary and a discussion of the cause of the neutron induced nuclear counter effect.

II. EXPERIMENT SETUP AND CALIBRATIONS

Fig. 1 shows the experimental setup used to measure the neutron induced nuclear counter effect with a pair of ^{252}Cf neutron sources. Each of these two ^{252}Cf sources weighs 4.4 μg. As shown in the figure, these two sources were separated by 14 cm and were mounted at the top of a Paraffin wax shielding with
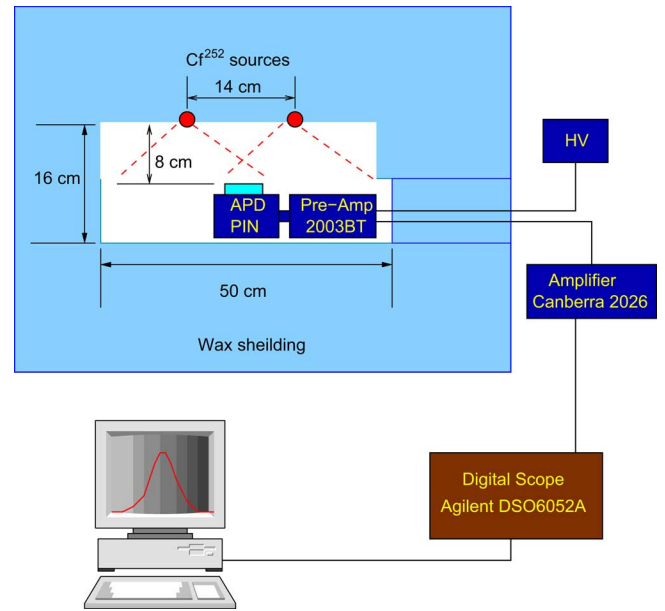

Fig. 1.   The experimental setup using a pair of ^{252}Cf sources.

dimension of $50 \times 10 \times 16$ cm (L $\times$ W $\times$ H). The photo-detectors were placed at the bottom of the Paraffin wax shielding at 8 cm from these sources. The neutron flux at the surface of photo-detectors was calculated to be 1.4×10^4 n/cm^2/s taking into account the ^{252}Cf constant 2.311×10^6 n/s/μg, the distances between the sources and the detector and the time since the delivery ($\tau_{1/2} = 2.6$ yr). A similar setup using one ^{241}Am $-$ Be neutron source was used for background study. In the ^{241}Am $-$ Be setup the photo-detectors were placed 2 cm away from the source. The neutron flux at the surface of the photo-detectors was calculated to be 6×10^4 n/cm^2/s taking into account the NIST certified fast neutron flux (NIST Test No 846/257817-93), the distances between the source and the detector and the time since the calibration ($\tau_{1/2} = 432$ yr). The high flux of the ^{241}Am $-$ Be neutron source allows a reduced data taking time for background runs.

Unless specified all irradiations were carried out with the front face of the photo-detectors facing the neutron sources. In both setups the signals from the photo-detectors were integrated by a Canberra 2003 BT pre-amplifier and shaped by a Canberra 2026 shaping amplifier before being sent to an Agilent 6052A digital storage oscilloscope. Data were taken with the scope operated in a self-trigger mode with threshold set at 1.5×10^5 electrons for APDs and 3.5×10^5 electrons for PIN diodes, allowing effective data taking to cover the high end of the pulse hight spectra. The silicon photo-detectors were reverse biased during the measurements, so that the PIN diode was fully depleted and the pair of APDs were set at a defined gain, e.g., 1, 10, 35, 100 and 200, while the nominal gain of these APDs in the CMS ECAL is 50. Because of the dark current and the large protection resistor in the Canberra 2003 BT pre-amplifier, the bias voltage from the power supply is different from that on the APDs. Unless specified, the bias voltage quoted in this text is the value applied to the pre-amplifier, which is larger than that on the APDs.
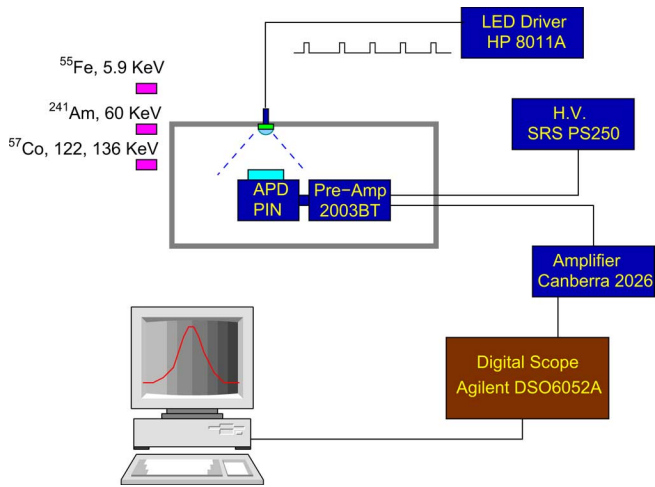
Fig. 2. The photo-detector calibration setup using a pulsed blue LED as well as ^{55}Fe, ^{241}Am and ^{57}Co x-ray sources.
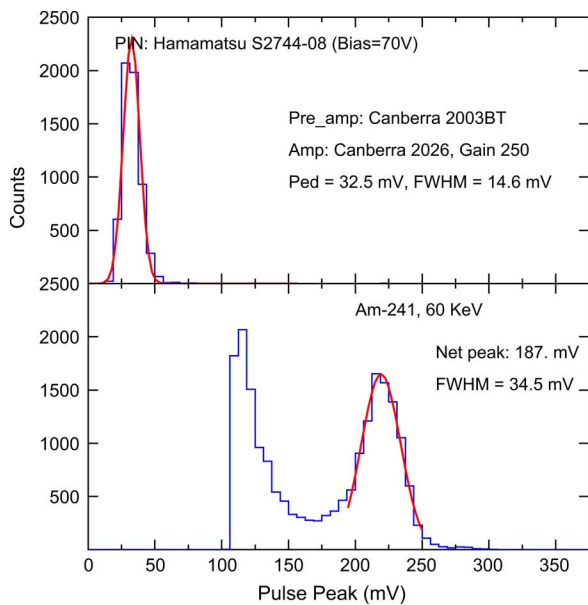

Fig. 3. The pedestal (top) and the pulse height spectrum of 60 keV X-rays from a ^{241}Am source (bottom) are shown for the Hamamatsu S2744-08 PIN diode.
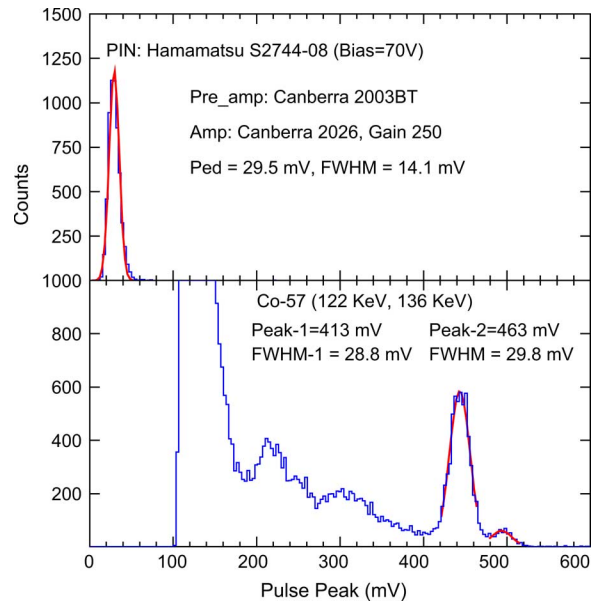

Fig. 4. The pedestal (top) and the pulse height spectrum of 122 keV and 136 keV γ-rays from a ^{57}Co source (bottom) are shown for the Hamamatsu S2744-08 PIN diode.
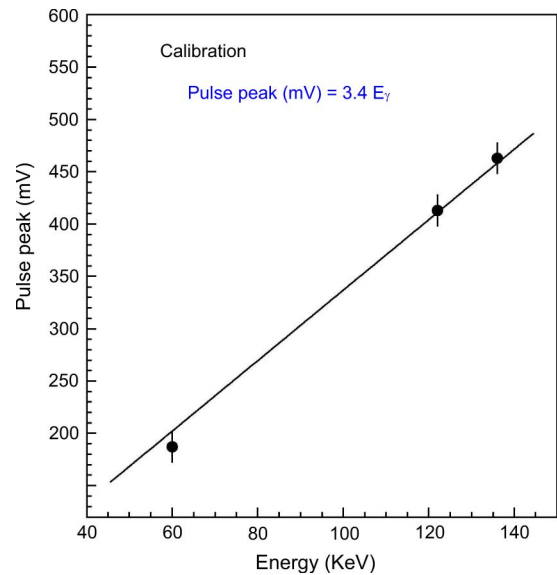

Fig. 5. The peak values (in mV) of the pulse height spectra are shown as a function of the source energy (in keV) and a linear fit for the Hamamatsu S2744-08 PIN diode.

The ^{252}Cf sources provide fast neutrons with kinetic energy peaked at 2.2 MeV with a tail up to 10 MeV [10]. The peak kinetic energy of these neutrons match well with the fast neutrons produced in particle showers [4], [5]. The energy spectrum of the ^{241}Am − Be source has a broad distribution from 2 to 10 MeV with an average kinetic energy of about 4.5 MeV [10].

Fig. 2 shows the calibration setup for the Hamamatsu PIN diode and APDs. The absolute electron numbers in these devices were calibrated by using peaks of x-ray or low energy γ-ray sources: ^{55}Fe (5.9 KeV) for the APDs and ^{241}Am (60 KeV) and ^{57}Co (122, 136 KeV) for the PIN diode.

Calibration of the PIN diode is straight forward. The top plots of Figs. 3 and 4 show pedestal distributions for the Hamamatsu S2744-08 photo-diode and the corresponding Gaussian fits. The bottom plots show the pulse height spectra obtained using a ^{241}Am source and a ^{57}Co source respectively. The corresponding peak ADC values for 60 keV, 122 keV and 136 keV

shown in these figures were determined by Gaussian fits and with pedestal subtracted. Assuming 3.62 eV energy deposition is needed to create an electron–hole pair in the silicon device these peak values were used to extract the calibration constants of equivalent electron numbers per mV pulse height for the PIN diode. The calibrations constants obtained from these three peaks are consistent, as shown in Fig. 5.

Calibrations for the APDs are more complicated. Fig. 6 shows the APD gain as a function of the bias voltage applied to the Canberra 2003 BT pre-amplifier. As discussed before that this bias voltage is larger than that on the APDs because of the dark current and the protection resistor in the pre-amplifier. The APD gain was measured with the pulsed blue LED light as shown in
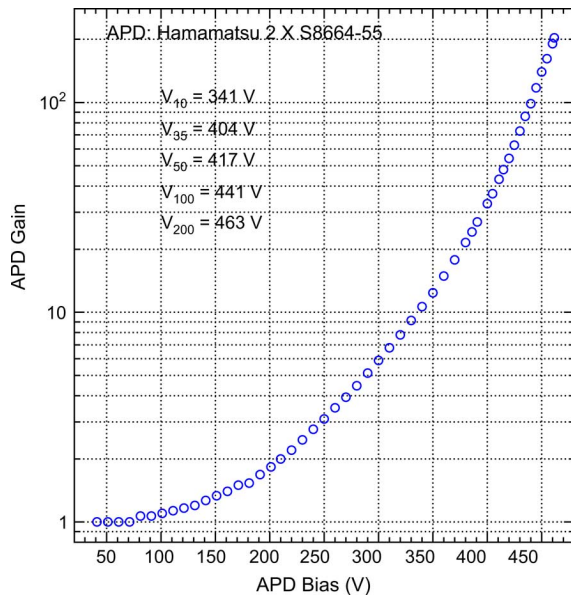
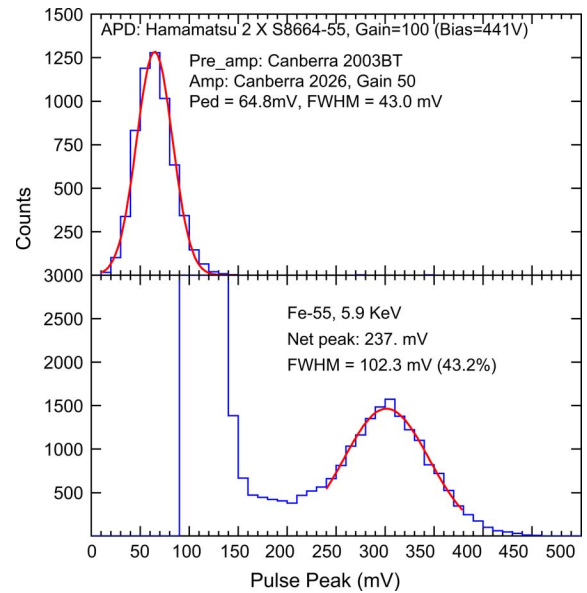Fig. 6. The APD gain is shown as a function of the bias applied to the Canberra 2003 BT pre-amplifier.

Fig. 7. The pulse height spectra of the pedestal (top) and the 5.9 keV X-rays from a ^{55}Fe source (bottom) are shown for the Hamamatsu S8664-55 APDs.

Fig. 2. Since this is a relative measurement no specific knowledge of the photon numbers per LED pulse was required.

Fig. 7 shows the pulse height spectra measured by the Hamamatsu S8644-55 APDs obtained by irradiating 5.9 keV X-ray from a ^{55}Fe source directly at the APDs. The APDs were reverse biased to set at a gain of 100. Similar calibration runs were carried out for the APD gains of 1, 10, 35 and 200. Like Figs. 3 and 4, the top plot of Fig. 7 shows a pedestal spectrum and a Gaussian fit. The bottom plot shows the spectrum taken with the ^{55}Fe source. It is known that when the reverse bias increases a fraction of the X-ray energies deposited inside the APDs does not receive the same amplification as scintillation photons would be [11]. Fig. 8 shows the ratio between the APD responses to 5.9 keV X-ray and to blue LED pulses as a function of the reverse bias applied to the APDs, which was used as the correction factors for the APD calibration at different gains. Once again no specific knowledge of the photon numbers per LED pulse was required in measuring these corrections since it is also a relative measurement.
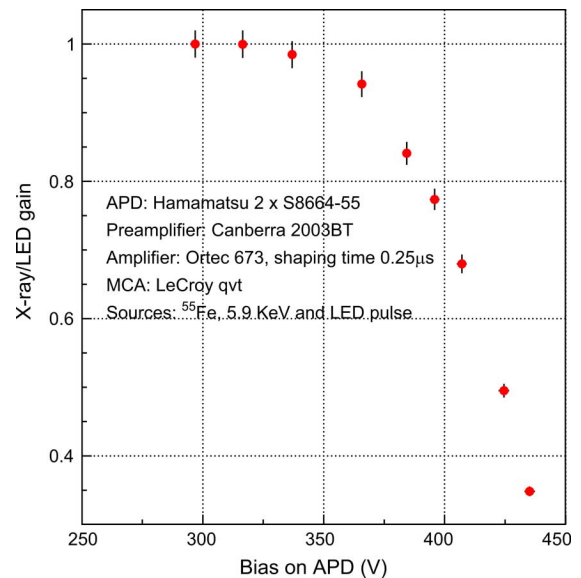

Fig. 8. The correction factors used for the APD calibrations with 5.9 keV X-rays are shown as a function of the reverse bias voltage applied on the APDs.

III. NEUTRON INDUCED NUCLEAR COUNTER EFFECT IN APDS AND PIN DIODES

Fig. 9 shows the pulse height spectra measured by two S8664-55 APDs for MeV neutrons from the ^{252}Cf sources. The horizontal scale is electron numbers determined according to the calibrations described in Section II. These electron numbers can be converted to equivalent energy deposition of scintillation photons according to the light output of the calorimeter, e.g., 4 p.e./MeV and 800 p.e./MeV respectively for PWO and LSO/LYSO crystals. Consistent spectra were observed in two runs lasting 91.5 h (dashes) and 62.1 h (dots). The sum of the spectrum (solid) represents a total run time of 154 h. Signals up to 2.2×10^6 electrons, corresponding to 8 MeV energy deposition in the sensitive layer of the APDs, are observed. A

few ten overflow events caused by amplifier saturation are also noticed for these spectra taken with the APD gain of 35.

Fig. 10 shows a comparison of the pulse height spectra measured by two S8664-55 APDs at various gains (solid: 10, dashes: 35, dots: 100 and dotted dashes: 200), for fast neutrons from the ^{252}Cf source. Signals of up to 2.5×10^6 electrons are observed for the APD gain of 10 without overflow, indicating up to 9 MeV energy deposition. Overflow events caused by amplifier saturation are observed for gains of 35, 100 and 200. The corresponding fractions of events with signals of more than 1.5×10^5 electrons is 1.6, 1.5, 0.28 and 0.27×10^{-6} respectively for the APD gains of 10, 35, 100 and 200, indicating that a high APD gain reduces the neutron-induced nuclear counter effect in the APDs. This observation is easy to understand: when the gain
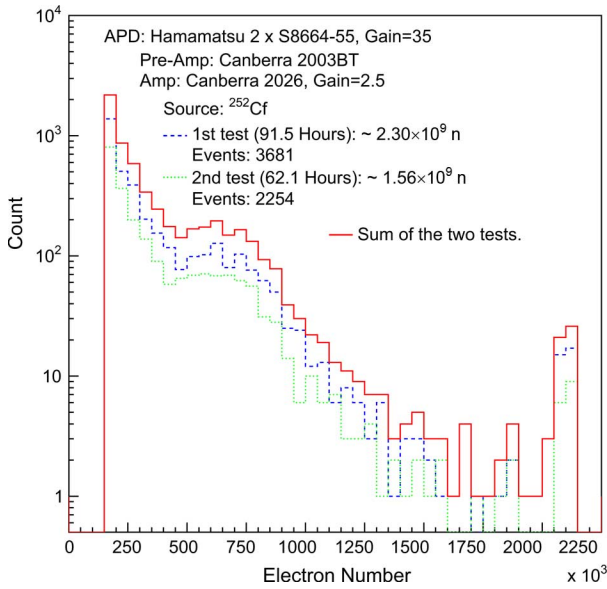
Fig. 9. Two pulse height spectra (dashes and dots) and their sum (solid) observed by the APDs under irradiation with MeV neutrons from the ^{252}Cf source pair are shown as a function of electron numbers.
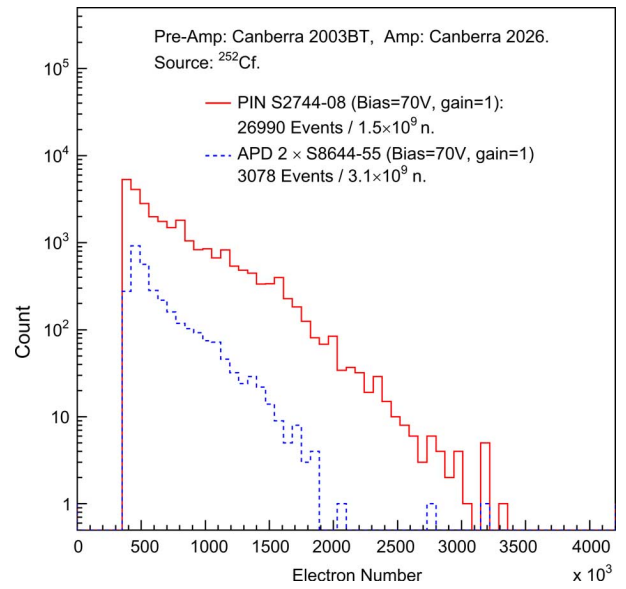

Fig. 11. Pulse height spectra in electron numbers, observed in the Hamamatsu S2744-08 PIN diode (solid) and the pair of Hamamatsu S8664-55 APDs (dashes), under irradiation by MeV neutrons from the ^{252}Cf source pair to the front face of the photo-detector.
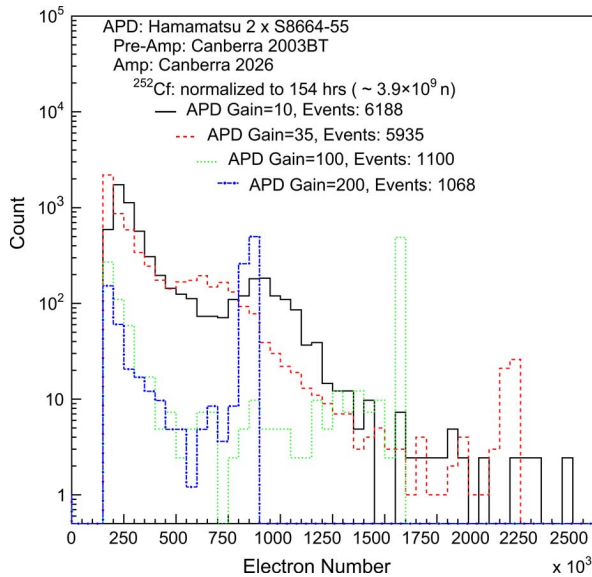

Fig. 10. The pulse height spectra in electron numbers observed by the APDs under irradiation with MeV neutrons from the ^{252}Cf source pair are shown for APD gains of 10 (solid), 35 (dashes), 100 (dots) and 200 (dotted dashes).

increases the electron signals induced by neutrons deep in the APDs receive a reduced amplification as compared to scintillation photons.

Fig. 11 compares the pulse height spectra measured by the pair of S8664-55 APDs (dashes) and the S2744-08 PIN diode (solid) for fast neutrons from the ^{252}Cf source. The irradiations were carried out with the front face of the photo-detectors facing the neutron sources. For this test the gain of the S8664-55 APDs was set at one with 70 V bias. Signals up to 2.5 and 3.0×10^6 electrons are observed for APDs and PIN diodes respectively. The high endpoint is observed for the S2744-08 PIN diode since it has a significantly thicker active layer than the S8664-55 APDs. The fraction of events with signals of more

than 3.5×10^5 electrons is 18 and 1.0×10^{-6} for the PIN diode and APDs respectively, indicating that the neutron-induced nuclear counter effect in APDs is more than an order of magnitude smaller than that in PIN diodes. It is clear that neutron induced nuclear counter effect can be reduced by using thin photo-detectors. In other words, a thick silicon photo-detector would be more effective as a neutron sensor.

It was suspected that the $500\,\mu$m thick epoxy resin at the front of these photo-detectors play an important role for the neutron induced nuclear counter effect since a low mass nucleus is an effective neutron moderator. It is well known that the maximum fraction of energy lost in a single elastic collision depends on the mass of the nucleus. It is ranged from 100% for ^1_1H to 1.7% for $^{238}_{92}U$. Fig. 12 shows pulse height spectra similar to Fig. 11 but with the back face of the photo-detectors facing the neutron sources. It is interesting to note that the fraction of events with signals of more than 3.5×10^5 electrons is 64 and 4.2×10^{-6} respectively for the PIN diode and the APDs, which is about a factor of four of what observed with the front face of the photo-detectors facing the sources. Since the thickness of the epoxy layers is $500\,\mu$m at the front but only a few ten μm at the back of these photo-detectors [9] this observation shows clearly that the $500\,\mu$m thick epoxy layers at the front of these devices do not enhance the neutron induced nuclear counter effect. A further measurement with an additional layer of epoxy of about $500\,\mu$m thick pasted at the front of a S2744-08 PIN diode also shows a reduction of the nuclear counter effect by about 10%.

To further investigate the effect of materials at the front of these photo-detectors various materials were inserted between these photo-detectors and the neutron source. Fig. 13 shows the pulse height spectra of the Hamamatsu S2744-08 PIN diode for MeV neutrons from the ^{252}Cf source pair with various materials of about 1 to 2 cm thick inserted in front of the PIN diode. The observed spectra have overall consistent shape, indicating that
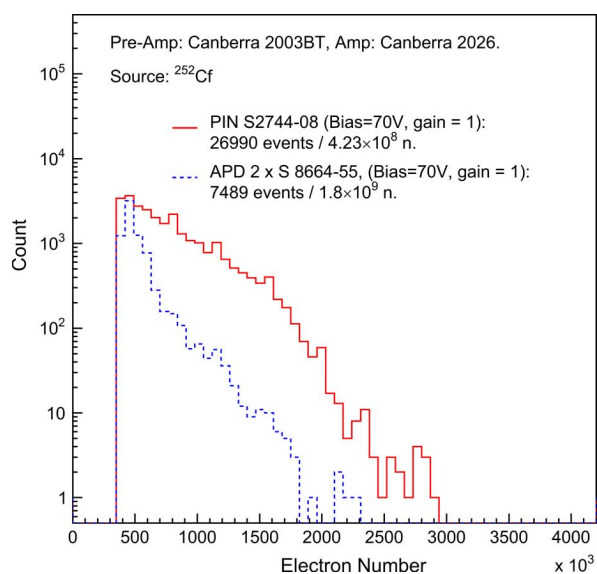
Fig. 12.   Pulse height spectra in electron numbers, observed in the Hamamatsu S2744-08 PIN diode (solid) and the pair of Hamamatsu S8664-55 APDs (dashes), under irradiation by MeV neutrons from the ^{252}Cf source pair to the back face of the photo-detector.

Fig. 14.   A comparison of the pulse height spectra in electron numbers, observed in the pair of Hamamatsu S8664-55 APDs under irradiation by MeV neutrons from the ^{252}Cf source (solid) and MeV γ-rays from a ^{60}Co source (dashes).
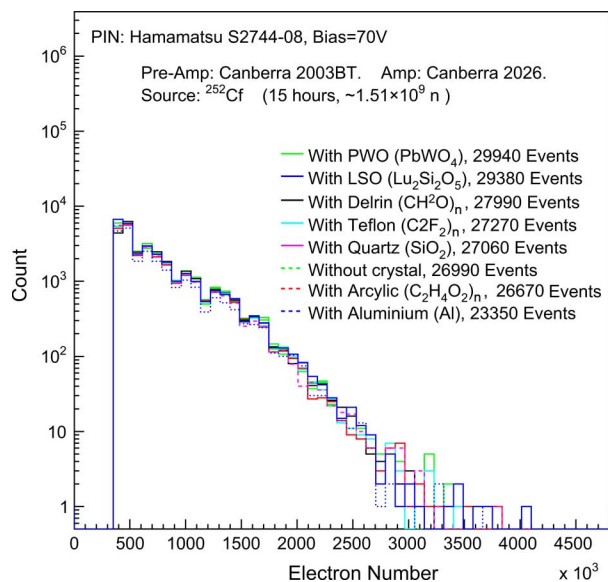

Fig. 13.   Pulse height spectra in electron numbers, observed in the Hamamatsu S2744-08 PIN diode under irradiation by MeV neutrons from the ^{252}Cf source pair with various materials inserted in front of the PIN diode.
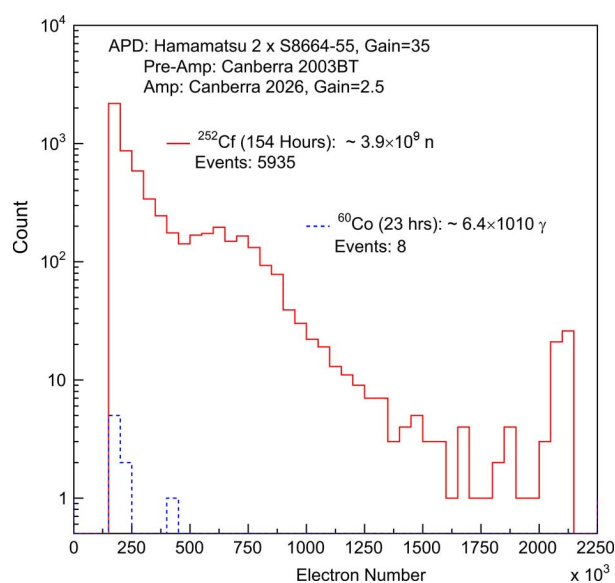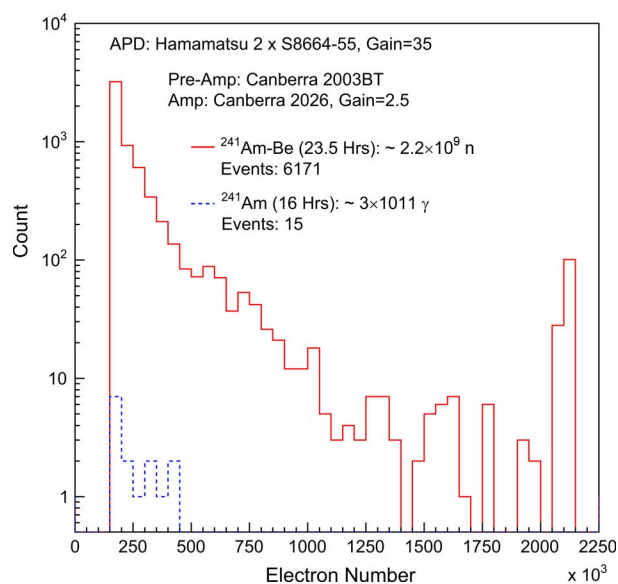

Fig. 15.   A comparison of the pulse height spectra in electron numbers, observed in the pair of Hamamatsu S8664-55 APDs under irradiation by MeV neutrons from a ^{241}Am $-$ Be source (solid) and 60 keV X-rays from a ^{241}Am source (dashes).

1 to 2 cm thick materials inserted have only a minor effect on fast neutrons as expected. The fraction of events with signals of more than 3.5×10^5 electrons, however, shows that the high Z materials, such as PWO and LSO, enhance slightly the neutron induced nuclear counter effect, while the low Z materials, such as H, C, O and Al, reduce slightly the effect. This observation is consistent with what was discussed above and reflects the fact that low Z material is a more effective moderator for fast neutrons.

1 MeV γ-rays from a ^{60}Co source and 60 keV X-rays from a ^{241}Am source were used to check possible background effect. Figs. 14 and 15 show the pulse height spectra measured by the

pair of S8664-55 APDs for fast neutrons from the ^{252}Cf source pair and the ^{241}Am $-$ Be source respectively. Also shown in these figures are pulse height spectra measured by the APDs for the 1 MeV γ-rays from a ^{60}Co source and the 60 keV X-rays from a ^{241}Am source. While the fractions of events with signals of more than 1.5×10^5 electrons are 1.5 and 2.8×10^{-6} for the ^{252}Cf source and the ^{241}Am $-$ Be source respectively, they are 13 and 5×10^{-11} for the ^{60}Co source and the ^{241}Am source respectively. It is clear contributions of X-rays and γ-rays are negligible in the spectra shown in Figs. 9–13. Similarly, replacing photo-detectors with a capacitance showed no counting in pulse
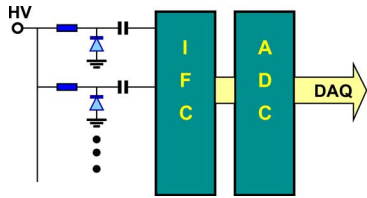
Fig. 16. The proposed scheme to eliminate the neutron induced nuclear counter effect using multiple readout devices and an intelligent front end chip.

heigh spectrum indicating that these spectra are entirely produced by the photo-detectors with no contamination from the readout electronics.

IV. PROPOSED SOLUTION

As discussed in Section I, the contamination in calorimeter data by neutron induced nuclear counter effect may be reduced by using event topology based rejection, where isolation, shower shape and event timing may be used [7]. However, it is clear that a complete elimination would need multiple readout channels for a single calorimeter cell. Two photo-detectors mounted on a single calorimeter cell with independent readout, for example, would provide two signals of equal amplitude for normal events generated by scintillation photons. When a difference is observed between these two signals the signal with a larger amplitude can be identified as being contaminated by nuclear counter effect and can be discarded. Doing so would preserve valid data for the calorimeter cell and eliminate nuclear counter effect completely. Implementation of multiple readout channels for a single calorimeter cell, however, increases the overall calorimeter cost. Existing calorimeters do have multiple photo-detectors for single calorimeter cell, but do not have multiple independent readout channels to conserve channel counting.

Fig. 16 is a schematic showing a proposed readout scheme using multiple photo-detectors. In this scheme an intelligent front-end chip compares signals from different photo-detectors and feeds only the ones not contaminated for digitization. By using this scheme the nuclear counter effect would be eliminated completely without increasing the total channel counting. Intelligent front-end chips with such capacity are a standard in modern calorimeter readout design, where comparators and amplifiers are integrated in the chip to provide an extended dynamic range of 10^5. Integration of additional comparators and selected readouts in such a chip is straight forward. Solutions along this line are discussed in the proposed CMS upgrade technical proposal [12] and are also expected to be implemented in the design for the proposed SuperB LSO/LYSO endcap calorimeter [6].

V. CONCLUSIONS AND DISCUSSIONS

Fast neutrons from ^{252}Cf source induce signals of up to several million electrons in Hamamatsu silicon APDs and PIN diodes causing neutron induced nuclear counter effect. This effect is believed to be realized in a two step process in the bulk silicon of these photo-detectors. In the first step fast neutrons lose a fraction of their kinetic energy to nuclei through elastic neutron-nucleus collisions with a cross section up to

10 barns. In the second step the charged nuclei deposit their kinetic energies in photo-detectors through ionization, which are converted into electron signals. The average number of elastic scattering collisions needed for a 2 MeV neutron to slow down to thermal energies, for example, ranges from 18 for $_1^1H$ to > 2000 for $_{92}^{238}U$. Multiple collisions occur between a fast neutron and several nuclei in the photo-detectors, leading to the end point of the observed spectra. On the other hand, the absorption cross-sections, such as (n,p) and (n, α), are more than five orders of magnitude lower than the elastic collisions for fast neutrons. The absorption process would play a major role when the neutrons are slowed down to thermal energies. Our data show that the $500~\mu$m thick epoxy coating at the front of these photo-detectors does not enhance the neutron induced nuclear counter effect. Our data also show that a low Z material at the front of these photo-detectors reduces the neutron induced nuclear counter effect.

The equivalent energy of the neutron induced nuclear counter effect in a crystal calorimeter depends on the crystal light yield. Anomalous signals of 2.5 million electrons, for example, correspond to 625 GeV and 3.1 GeV for PWO and LSO/LYSO crystals respectively assuming the light yields of 4 and 800 p.e./MeV for calorimeter size crystals. As discussed in Section I, the impact of such signals on the physics output is comparable between the CMS PWO calorimeter at the LHC and the proposed SuperB forward LSO/LYSO calorimeter at the proposed SuperB collider. The rate of the neutron induced nuclear counter effect in APDs is more than an order of magnitude lower than that in PIN diodes, indicating that APD is a preferred photo-detector in this aspect. Increasing the APD gain also reduces the effect. All these are due to the fact that only a portion of the neutron induced electron signals in the APDs receives full multiplication.

The neutron induced nuclear counter effect may be reduced by advanced data analysis by using event topology based selection. Its complete elimination requires multiple readout channels for a single calorimeter cell. An intelligent front-end chip with multiple photo-detectors is proposed to provide this function without requiring multiple readout channels for a single calorimeter cell and thus leading to a significant cost saving for future calorimeters designed to be immune to the nuclear counter effect.

REFERENCES

[1] A. Satpathy, K. Tamai, M. Fukushima, D. Y. Kim, and M. H. Lee, "Nuclear counter effect of silicon pin photo-diode used in CsI(Tl) calorimeter," *Nucl. Instr. Meth.*, vol. A391, pp. 423–426, 1997.

[2] T. Kirn, Y. Musienko, T. Flugel, and D. Renker, "Performance of the most recent Hamamatsu avalanche photo-diode," *Nucl. Instr. Meth.*, vol. A387, pp. 199–201, 1997.

[3] Y. Hosono, S. Sjafruddin, T. Iguchi, and M. Nakazawa, "Fast neutron detector using PIN-type silicon photo-diode," *Nucl. Instr. Meth.*, vol. A361, pp. 554–557, 1995.

[4] The CMS Collaboration The CMS Electromagnetic Calorimeter Project, CERN/LHCC 97-33, 1997.

[5] "Radioactivity and Radiation Protection, Section 29 of the Review of Particle Physics," *Phys.Lett*, vol. B667, 2008.

[6] C. Cecchi, "A LYSO calorimeter for a superB factory," in *Proc. 14th Int. Conf. Calorimetry in Particle Physics, Journal of Physics Series*, 2010 [Online]. Available: http://indico.ihep.ac.cn/get-File.py/access?contribId=266&sessionId=15&resId=0&material-Id=slides&confId=910

[7] The CMS Collaboration, Electromagnetic Calorimeter Commissioning and First Results with 7 TeV Data, CMS Note 2010-012 in CERN Document System. [Online]. Available: http://cdsweb.cern.ch/record/1278160?ln=en

[8] K. Deiters *et al.*, "Properties of the most recent avalanche photo-diodes for the CMS electromagnetic calorimeter," *Nucl. Instr. Meth.*, vol. A442, pp. 193–197, 2000.

[9] T. Zarzycki, private communication.

[10] S.-T. Park, "Neutron energy spectra of ^{252}Cf, Am-Be source and of the D(d,n) ^{3}He reaction," *J. Rad. Nucl. Chem.*, vol. 256, pp. 163–166, 2003.

[11] J. M. Chen, R. H. Mao, L. Y. Zhang, and R.-Y. Zhu, "Large size LSO and LYSO crystals for future high energy physics experiments," *IEEE Trans. Nucl. Sci.*, vol. 54, no. 3, pp. 718–724, Apr. 2007.

[12] The CMS Collaboration, Technical Proposal for the Upgrade of the CMS Detector Through 2020 CMS U1TDR, 2011.